

Cite this: *Nanoscale*, 2012, **4**, 3820

www.rsc.org/nanoscale

REVIEW

As flat as it gets: ultrasmooth surfaces from template-stripping procedures

Nicolas Vogel,^{*a} Julius Zieleniecki^b and Ingo Köper^b

Received 24th February 2012, Accepted 23rd April 2012

DOI: 10.1039/c2nr30434a

In an experimentally simple replica process, the natural flatness of mica or polished silicon wafers can be transferred to metal films, resulting in metal surfaces with topographic features in Angstrom dimensions over large areas. Two decades after its invention, the template-stripping process continues to appeal to scientists from diverse research backgrounds primarily due to its simplicity, cost-effectiveness and ability to yield high quality substrates and structures. This article introduces the basic construction process for template-stripped substrates, and reports on a variety of extensions of the process, including the generation of materials contrasts and the design of tailored topographies. It also highlights the use of such substrates in a variety of research fields in nanoscience and technology ranging from surface force measurement and high definition imaging to the self-assembly of model membranes and plasmonics.

1. Introduction

Research and technology are continuously pushing towards the nanoscale, with more and more applications exploiting the special properties of ultrathin films, assemblies of molecular monolayers and even molecules themselves. Self-organization of

molecules into functional superstructures is one of the key processes for the realization of state-of-the-art devices.

In order to investigate, characterize and use surface bound processes and assemblies at the nanoscale, extremely smooth substrate surfaces are required. In general, the roughness of the surface needs to be of smaller dimensions than those of the molecules or structures under investigation, in order to guarantee reliable measurement conditions or device performances. For example, the imaging of molecules or molecular assemblies using Atomic Force Microscopy (AFM) or Scanning Tunneling Microscopy (STM) requires smooth surfaces to yield accurate height information.^{1–3} Similarly, the measurement of surface forces is extremely sensitive to substrate inhomogeneities.^{4,23}

^aSchool of Engineering and Applied Sciences, Harvard University, 29 Oxford Street, Cambridge, MA 02138, USA. E-mail: nvogel@seas.harvard.edu

^bFlinders Centre for NanoScale Science and Technology, School of Chemical and Physical Sciences, Flinders University, GPO Box 2100, Adelaide, SA 5001, Australia. E-mail: ingo.koepfer@flinders.edu.au



Nicolas Vogel

Nicolas Vogel studied chemistry at the University of Mainz, Germany and at Seoul National University, South Korea and conducted research for his diploma thesis in the group of Wolfgang Knoll at the Max Planck Institute for Polymer Research in Mainz, Germany. For his PhD, he joined Katharina Landfester's group at the Max Planck Institute to work on two dimensional colloidal crystallization and colloidal lithography. He received his PhD in

2011 and is currently staying in the group of Joanna Aizenberg at Harvard University.



Julius Zieleniecki

Julius Zieleniecki studied Nanotechnology at the Flinders University, Adelaide, Australia. He received his Honours in 2011 and then was awarded a fellowship to conduct his PhD. His research is focussed on membrane–drug interactions.

The assembly of functional superstructures is another example where smooth substrate properties are essential. The formation of solid supported lipid membranes to study membrane related processes requires a well-ordered assembly of phospholipid molecules.⁵⁻⁷ Similarly, monolayer-based devices, *e.g.* in optoelectronic applications, depend on the extended stacking of molecules with high precision therefore demanding substrates with a roughness basically smaller than the dimensions of the molecules.⁸

The choice of such smooth surfaces however is limited. Several materials inherently possess extremely smooth surfaces. Prominent examples are silicon wafers that can be polished along their crystal axis or the silicate mica, consisting of layered structures that can be cleaved individually yielding atomically flat substrates. Unfortunately, the insulating character of these materials impedes their use as substrates for electrochemical investigations or STM. For such applications, conducting and chemically relatively inert gold surfaces are ideal. Additionally, the strong binding of thiol moieties to gold offers easy access to various surface modifications. However, since gold films typically grow under the formation of islands, the roughness of such films is usually too high.

For various nanotechnological applications, the combination of the flatness of mica or silicon with the materials properties of gold is highly desirable. Following a process originally utilized to embed biomolecules into carbon film by Butt,¹ Butt² and Hegner³ transferred the methodology to gold films in 1993 to come up with a template stripping process to transfer the low surface roughness of mica to a gold surface. The basic principle and some recent applications of this process will be reviewed in this article. The process has started to attract attention from a wide field of nanotechnology related applications due to its simplicity, robustness and precision in substrate engineering with an increasing number of substrate materials that can be applied.

First, the 'classical' template stripping process, leading to homogeneous, ultrasmooth metal films is examined in detail and refinements of the technique with respect to accessible surface

materials, bonding techniques and mechanical supports are introduced. Then, more sophisticated processes leading to patterned, ultrasmooth substrates are presented. Chemical patterning, leading to topography-less substrates consisting of two different surface materials that are smoothly connected to form a homogeneous surface has been shown to be an interesting approach to create nanoscale patterns of self-assembled monolayers. Physical patterning, leading to homogeneous, ultrasmooth metal films with defined topographies is another recent development towards functional, high quality metal films that can be used for example for low-loss plasmonic applications.

In the last part, various applications of template stripped surfaces are presented to highlight the high precision and versatility of the process.

2. Preparation of smooth homogeneous metal films

The Template Stripping (TS) process is schematically shown in Fig. 1 using gold as an example to create an ultra-flat surface. A template is used to produce a homogeneous, ultra-flat gold film. First, a thin gold film is deposited onto the smooth template surface. Thermal evaporation or sputtering processes usually lead to relatively rough surfaces. Subsequently, an adhesion layer is added on top of the gold surface to attach a solid support (typically a glass slide) onto the gold layer. Typically, two component, thermally curable epoxy resins are used as the adhesion layer.⁹ Finally, the sandwich structure can be mechanically cleaved at the point of weakest adhesion. Due to the lattice mismatch between gold and the template material, the cleavage will occur at the Si–Au interface, leading to the release of the gold interface with a roughness similar to the template.

The process allows for the preparation of extremely smooth gold surfaces over large areas. Compared to commercially available Au[111] substrates or flame annealed substrates with atomically flat gold terraces, the TS procedure yields substrates of arbitrary large areas only limited by the dimensions of the template material. The surfaces are not atomically flat, but rather present a smooth, amorphous surface without any terraces or steps. An attractive additional benefit is the ability to store the sandwiched structures without inducing damage or contamination to the gold surface as the latter is hidden in the sandwiched layers without being exposed to ambient conditions. A fresh gold surface can be cleaved on demand from the sandwiched precursor. As metal surfaces are known to get contaminated easily in environmental conditions by oxygen, thiol compounds or hydrocarbons,^{10,11} the on-demand cleavage can be of crucial importance for reliable high precision measurements on

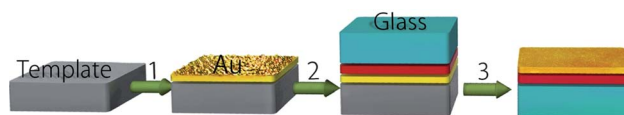


Fig. 1 Schematic illustration of the template stripping process with gold as a material's example. Onto a naturally flat template, a thin gold film is thermally evaporated. A mechanical support is glued onto the gold film. Cleavage can be induced at the weakest point of adhesion between gold and the template, leading to a gold surface with a roughness comparable to the template.



Ingo Köper

Ingo Köper studied chemistry at the University of Dortmund and received his Diploma in 1998. In 2002 he received his PhD from the University of Paris VI for his work on neutron scattering. In 2002 he joined the Materials Science Department at the Max Planck Institute for Polymer Research, Mainz, Germany. After one year as a post-doc, he became a project leader, leading an independent research team working on biofunctional surfaces, ion channels and single-channel recordings. In

September 2009, he followed a call to become lecturer in the School of Chemical and Physical Sciences at Flinders University, Adelaide, Australia.

surfaces.¹² Additionally, large areas of extremely flat metal surfaces can be reliably generated in a cheap and straightforward fashion, thus making the process interesting for industrial applications as well; especially with templates that can be dissolved in the course of the process.

Since the first reports by Butt^{1,2} and Hegner,³ the TS procedure has been significantly extended with respect to the type of metal used, template materials as well as bonding techniques elaborated to overcome swelling and dissolution of impurities of the epoxy-resins when immersed in organic solvents.

Templates

Mica was the first material to be used as a template. It provides an atomically flat surface, which can be prepared by cleavage. However, its layer structure can induce problems during mechanical stripping as individual sheets of mica may not be removed during the delamination of the template.^{13,41,83} A significant advantage towards reliable, large scale production of pure gold films came from the use of polished silicon wafers as templates.¹⁴ With roughness comparable to mica, the mechanical stability of the wafer allows for the reliable stripping of the metal film without the risk of surface contaminations by traces of the template material. Therefore, the silicon wafer based template stripping method has become the standard technique in template-stripping based applications.^{5,7,8,15} Another benefit of using silicon as template material is the possibility to create patterns in the template by micromechanical engineering, thus leading to a physically patterned gold surface after cleavage.¹⁶ As an alternative to silicon, the use of gypsum was proposed. Gypsum can be cleaved easily at its [010] plane and offers a similarly smooth surface as silicon or mica.¹⁷ In contrast to the latter, the gypsum template can be removed by immersion in water without application of mechanical separation forces.¹⁷

An improvement of the quality of template stripped gold film in terms of avoiding pinholes¹⁸ and an increase in grain sizes has been reported for flame- and thermally annealed gold films.¹⁹ However, from the experience of the authors, no pinholes were found in template stripped gold films prepared without flame annealing. Naturally, difficulties arise when cleaving materials with a high adhesion to the template material of choice. It has been shown that the introduction of a very thin passivation layer can significantly reduce the adhesion, thus leading to rupture at the desired interface. Using a very thin layer of carbon allowed the successful cleavage of titanium dioxide and silicon dioxide from mica²² while the presence of a single layer of methyl groups introduced by self-assembling hexamethyldisilazane on a silicon wafer provided enough passivation to induce rupture between the silicon wafer and silicon dioxide.^{15,43}

Surface materials

Initially developed for gold, the TS procedure has been extended to a wider range of materials that can be cleaved from a template. Several different metals have been successfully used, including silver,^{12,20} platinum,^{10,12} palladium,¹² titanium,^{21,82,83} and nickel.¹³ The process has also been used with inorganic and organic materials such as titanium dioxide,²² carbon,²³ and polyaryletherketon.²⁴ The variety of materials that have been

successfully applied demonstrates the versatility of the approach. In general, the key requirement to prepare a template-stripped replica surface from an arbitrary material is to generate an interface with the lowest adhesion between template and surface material. The wide range of available template materials paired with the possibility to passivate the wafer by silanization opens various options to tune the adhesive properties in the system and leaves plenty of opportunities to extend the range of accessible materials according to a desired application.

Binding layer, mechanical support and separation protocols

Traditionally, epoxy resins have been used as adhesion layers to glue the metal film to a solid substrate. However, if the template stripped substrate is to be immersed in organic solvents, especially THF or toluene, partial swelling and dissolution of the epoxy film might compromise the smoothness of the film. Wagner *et al.*⁹ made a survey of commercially available glues and developed protocols for the successful application of different epoxy based glues (Epo-tek 377 and Epo-tek 301-2) as well as dental (*Panavia 21*) and inorganic adhesives (*Cerastil C7*). Weiss *et al.* reported the successful use of UV curable adhesives.¹² The molecular adhesion between gold and thiol molecules was used to bind the gold layer on a PDMS substrate modified with mercapto-silane moieties as a SAM-based adhesive.²⁵

Finally, the use of an adhesive layer can be completely avoided by using cold welding processes to directly bind the gold layer at elevated temperature and pressure to a second gold layer attached *via* a chromium or titanium adhesion promoter to a glass substrate.^{11,26} Similarly, electroplating a nickel support layer onto the gold can allow for template stripping the metallic film from the wafer template without any additional adhesive layer.^{20,27} Recently, a process modification has been reported that uses a silica precursor solution (“liquid glass”) as the mechanical support.⁸⁶ A chromium layer is evaporated onto the thermally evaporated gold film and plasma treated to enable wetting with the aqueous silica precursor solution. After curing at elevated temperatures, rupture is induced by bending the mica-template.

Overall, three distinct material classes have successfully been employed as supports. Traditionally, glass or Si-wafers have been used.^{1-3,9} The second class includes metallic supports which can be used to design conducting substrates *via* electroplating of nickel^{20,27} or gluing the film to a low melting solder that can be cast onto the gold film.¹² Thirdly, bendable template stripped metal films have been prepared using elastomeric PDMS substrates as mechanical support.^{12,25} It has been demonstrated that mechanical bending of the substrate slightly increases the roughness of a template stripped Ag film. However, even after bending, the roughness was still below values measured on thermally evaporated films.¹²

The separation of the template–gold interface can be achieved mechanically, typically by applying a razor blade to the edges of the sandwich structure.¹² An alternative is the chemical separation method that cleaves mica by immersion of the sandwich structure into thiol containing ethanolic solutions. The thiols can intercalate into the mica sheets and thus reduce the binding to the gold.²⁸ The procedure has been shown to be also applicable to silicon templates.¹²

Characterization of template stripped surfaces

Template stripped surfaces are usually characterized using AFM or STM. In comparison to thermally evaporated gold, the surface of template stripped gold shows a significantly reduced roughness (Fig. 2).

Fig. 2 shows AFM height images of a thermally evaporated (a) and a template stripped gold film (b) prepared from a silicon wafer template.²⁹ The island growths of gold during the evaporation process led to distinct gold domains resembling a hilly landscape. In contrast, the template stripped surface appears much smoother (please note the different z-scale) and the lack of grain structure is visible. The different morphology is further highlighted by line scans along the black line shown in the AFM images (Fig. 2c and d). A quantitative analysis of the AFM images shows an RMS roughness of 1.45 nm for the thermally evaporated gold film and 0.20 nm for the template stripped sample. The maximum peak-to-valley distances in the line scan are 7.4 nm and 1.1 nm, respectively.²⁹ Similar results have been obtained for several different metals (Ag, Au, Pd and Pt) (Fig. 2e).¹²

A detailed STM analysis comparing single crystalline Pt[111] and template stripped platinum showed that the latter consisted mostly of [111] facets and features of smaller domain sizes compared to the single crystalline surface. Nevertheless, the single crystalline sample featured more extended terrace structures that led to a higher total roughness than the template stripped sample.³⁰ In a detailed analysis on the stripping procedure, Borukhin and Pokroy recently demonstrated that the mechanical stress during the stripping procedure induces deformation defects in the gold film close to the stripping plane that could be prevented by using solvent assisted cleavage.³¹ Compared to thermally evaporated films, it has been shown that template stripped silver films possess much larger grain sizes.⁸

Recently, it was shown that thermal annealing can be used to significantly enlarge the crystallite sizes to produce samples with grain sizes extending up to square micrometers.³¹ Care has to be

taken to passivate the silicon wafer template prior to annealing to prevent diffusion of silicon atoms into the gold.

3. Preparation of patterned, ultrasmooth surfaces

In recent years, the template stripping procedure has been extended in order to produce laterally structured sample surfaces. Two distinct approaches have been developed. Chemically patterned samples consist of different materials that merge homogeneously into an ultra-smooth film without any surface topography. In contrast, physically patterned samples consist of one single material but feature topographies by pre-patterning of the template material. Both approaches have enabled the template stripping process to be applied in a variety of different applications (see below).

Chemical patterning: generation of material contrast

The original TS process leads to homogeneous metal films. However, various applications require heterogeneously structured samples. This includes distinct materials regions, for example electrodes surrounded by insulating parts or patterned functional compounds such as self-assembled monolayers. A variety of approaches to pattern self-assembled monolayers into superstructures have been proposed using microcontact printing^{32–34} or lithographic patterning of photosensitive silane molecules.^{35–37} However, if different parts of the substrates are to be addressed individually, the substrate itself has to be structured.

The combination of patterning processes with the TS protocols enables the preparation of ultrasmooth substrates that feature different surface materials and can thus be used for the site-selective self-assembly of functional molecules. Such a substrate allows for a very precise arrangement of multifunctional monolayers on substrate regions with defined materials properties, for example electrodes or insulators. The self-assembly of the different molecules will not be affected by

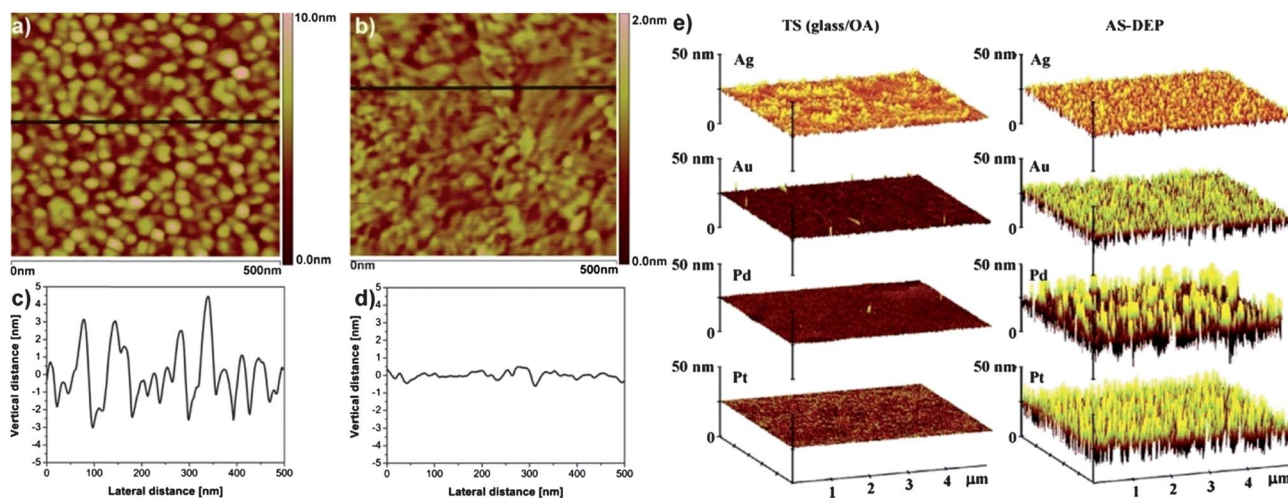


Fig. 2 Surface morphology of thermally evaporated and template stripped metal films. Reprinted from ref. 29 with permission from Elsevier. (a and b) AFM height images of a thermally evaporated 50 nm gold film (a) and a film with similar thickness prepared by the template stripping process (b). (c and d) Line scans along the black line shown in the images. (e) Comparison of the surface morphologies of different metal films prepared by template stripping (left side) and by thermal evaporation (right side). Reprinted with permission from ref. 12. Copyright 2007 American Chemical Society.

surface topographies, enabling device applications that exploit the properties of single molecular layers.

Colloidal lithography, where a colloidal monolayer serves as an evaporation mask, has been recognized as a cheap and efficient method to produce large patterned areas of nanostructures in a highly parallel fashion.^{38–40}

Frey *et al.*^{41,42} combined colloidal lithography on a mica template with a stripping process to produce laterally patterned surfaces comprised of different combinations of Au, Ag, Al and SiO₂ as surface materials but reported difficulties with mica residues on their substrate. A modification of the process reported by Vogel *et al.*^{15,43} makes use of a silicon wafer template for the heterogeneous patterning process.⁴³ The process is schematically shown in Fig. 3.¹⁵ The silicon wafer template is modified with hexamethyldisilazane to form a methyl monolayer that reduces the adhesion between the wafer template and silicon dioxide, which is evaporated in a later step of the process. A colloidal monolayer is assembled on the passivated wafer and thin layers of gold (50 nm) and chromium (<2 nm) are evaporated (Fig. 3a and b). The chromium layer serves as an adhesion promoter to silicon dioxide that is deposited in a second evaporation step after removal of the colloid mask (Fig. 3c and d). Finally, a glass slide is glued onto the modified template wafer

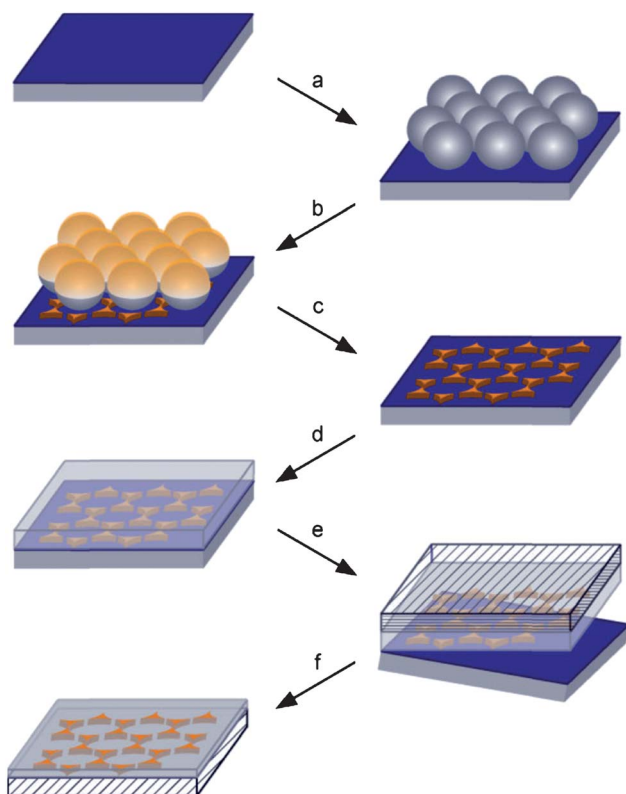


Fig. 3 Process flow to generate chemically patterned, ultraflat substrates.¹⁵ A hexamethyldisilazane-modified wafer is used as template material. (a) Colloidal monolayer assembly. (b) Thermal evaporation of gold (50 nm) and chromium (<2 nm). (c) Removal of the colloidal monolayer. (d) Thermal evaporation of silicon dioxide (100 nm). (e) Gluing of the interface to a glass slide and mechanical separation. (f) Template-stripped surface with gold nanoparticles embedded in a silicon dioxide matrix. Reprinted with permission from ref. 15.

using an epoxy glue. Mechanical cleavage removes the template wafer and reveals a laterally patterned, ultrasurface composed of gold nanotriangle arrays embedded in a silicon dioxide matrix (Fig. 3e and f). The two different substrate materials enable the selective modification of surface regions by thiol and silane chemistry. Furthermore the combination of conductive and insulating material allows for an electric addressing of designed surface regions.

The obtained surface has been characterized by AFM (Fig. 4). While the height image does not show any surface topography, a clear phase contrast due to the different hardness of the gold- and silicon dioxide surface regions can be seen. On a size of 25 μm^2 , an RMS roughness of 0.21 nm has been found, in excellent agreement with values reported for pure gold films.⁴³ The low roughness that is comparable to plain template stripped gold (compare Fig. 2b and d) is further underlined by a line scan along the black line of the height image shown in Fig. 4c. The maximum peak-to-valley difference is 0.8 nm.⁴³

The possibility to create defined monolayer domains at nanoscale dimensions is shown in Fig. 4d and e. It shows an AFM height image of a chemically patterned substrate with gold nanostructures that were selectively modified with hexadecanethiol. A line scan (Fig. 4e) shows the accurate grafting of the monolayer selectively on the gold nanopatches. The thiol monolayer height was measured to 1.5 nm, in complete agreement with the theoretical height.⁴³ Furthermore, a double functionalization of both silicon dioxide and gold patches was performed and visualized using a wettability contrast in micron-sized domains produced by using a TEM grid as a mask for patterning. The wettability pattern produced by cooling the sample to condense water onto the surface is shown in Fig. 4f. The gold regions (bright in the impinging illumination on the left side; dark in the transmission image of the right side) were turned hydrophilic by a hydroxyl thiol and feature big water droplets. The silicon dioxide part was rendered hydrophobic by an alkyl silane and showed very limited water condensation.⁴³

Adding additional sputtering deposition processes in colloidal lithography leads to nanostructures with larger sizes compared to thermal evaporation due to the less directed nature of the sputtering process. This has been used to combine the two metal deposition techniques with the template stripping procedure in order to produce ternary surface structures consisting of gold, titanium and cobalt surface regions with nanometer dimensions.⁴⁴

The demonstration of successful combinations of colloidal lithography with the TS procedure has to be seen as an important extension to both processes. It enables the creation of a wide range of surface embedded, ultra-smooth surface structures to suit any application aiming at a precise positioning of functional molecule arrangements on tailored surfaces.

Since the first report on colloidal lithography to create arrays of gold or silver nanotriangles,^{45,46} the field has been rapidly expanding and research efforts have led to an increase in the method's versatility.^{38,39,47} Especially the use of more complex colloidal arrangements such as binary⁴⁸ or non-close-packed colloidal arrangements⁴⁹ paired with sophisticated evaporation⁵⁰ and etching protocols⁵¹ has significantly increased the available structural designs. As examples, the design of arrays of nanoscale rings,⁵² discs or crescent shaped particles^{51,53,54} has been explored

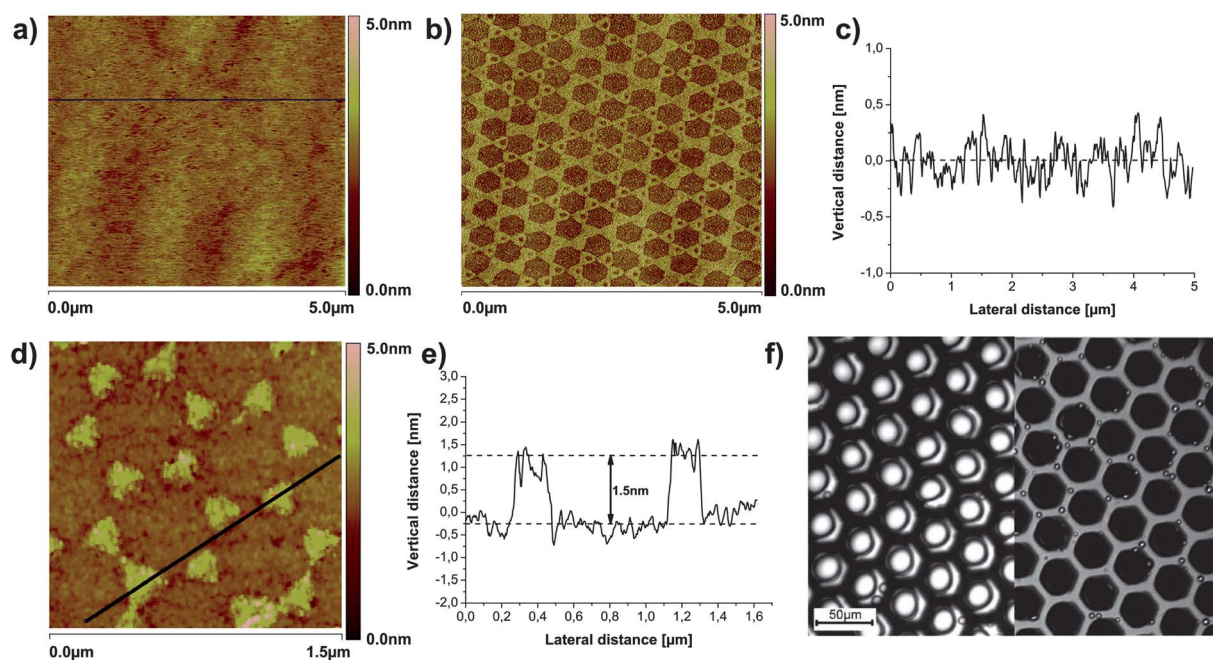


Fig. 4 Chemically patterned, heterogeneous surfaces consisting of gold and silicon dioxide. (a–c) AFM characterization of a pristine surface after template stripping. (a) AFM height image, (b) AFM phase image, (c) line scan along the black line shown in the height image. (d–f) Selective functionalization of the surface regions. (a) Nanoscale surface functionalization of gold triangles embedded in SiO₂ by self-assembly of hexadecanethiol. (e) Line scan along the black line of the height image. (f) Wettability contrast of a micropatterned surface induced by silanizing the silicon dioxide areas with alkyl-silanes and modifying the gold hexagonal structures with a carboxylic acid terminated thiol. Left side: impinging illumination (gold appears bright), right side: transmission illumination (gold appears dark). Reprinted with permission from ref. 43.

in detail. Furthermore, different surface materials such as magnetic compounds^{55,56} have been created. More recent processes also allow for the preparation of extremely small nanoparticle arrays, by the application of metal-complex precursor filled colloidal particles.^{57–60}

The large variety of available surface structuring protocols for various structures and materials has yet to be combined with template stripping procedures. In the future, an increase in applications aiming at the combination of ultra-smooth and high quality metal surfaces with a tailored design of nanostructures is anticipated.

Physical patterning: generation of defined topographies

A novel, conceptually different approach to obtain patterned, ultra-smooth surfaces by the template stripping procedure is illustrated in Fig. 5. A pre-patterned silicon wafer featuring the negative of the desired structures can be applied as template material.^{16,61–63}

The pattern is written into the silicon wafer employing standard nanofabrication techniques such as photo- or electron-beam lithography or a focused ion beam (Fig. 5a). A continuous gold film is subsequently evaporated onto the wafer template (b), glued on a backing layer (c) and mechanically cleaved from the wafer template. The inverse of the structural features of the wafer template is transferred on the template stripped surface (d). If the depth of the structures is deeper than the thickness of the evaporated gold, discontinuous films result after stripping (d, left structure). The silicon mold can be re-used. The possibility to create well-defined structures in a silicon wafer due to differences

in etching rates of different facets of the silicon crystal allows for the preparation of very smooth, high quality nanoscale features after template stripping. Fig. 5e–l illustrates examples from the recent literature. Nagpal *et al.* demonstrated stripping of arrayed objects such as nanohole films (e), pyramids (f) or concentric rings termed bull's eye structures (g).¹⁶ The nanohole arrays are an example of a discontinuous gold film prepared by milling deep holes into the wafer. Subsequent gold evaporation will not be sufficient to form a continuous film on the wafer. After stripping, the holes milled into the wafer will be transferred to holes in the template stripped surface.

Zhu *et al.* fabricated differently shaped plasmonic nanocavities consisting of defined silver nanostructures arranged in a way as to form a cavity in their middle.⁶³ This cavity can be triangular shaped (Fig. 5h), round (i), or a whispering gallery structure (j). A further increase in versatility of the template stripping process was achieved by the introduction of nanoscale features above the silicon wafer template. The fabrication of freestanding nanoscale grooves were reported by Lindquist *et al.* who visualized a clear distinction between the rough (evaporated) side of the freestanding film (Fig. 5k) and the template stripped, smooth side (Fig. 5l).⁶² By a combination of focused ion beam milling with deposition of platinum nanostructures onto the template wafer, the fabrication of ultra-flat gold surfaces with simultaneous concave and convex features became feasible.⁶²

The template stripping process also allows for the embedding of dielectric cavities into an ultra-flat metal film as demonstrated by Kho and co-workers.⁶⁴ Such high quality metal nanostructures find applications in modern plasmonics as their low surface roughness effectively prevents losses from undefined

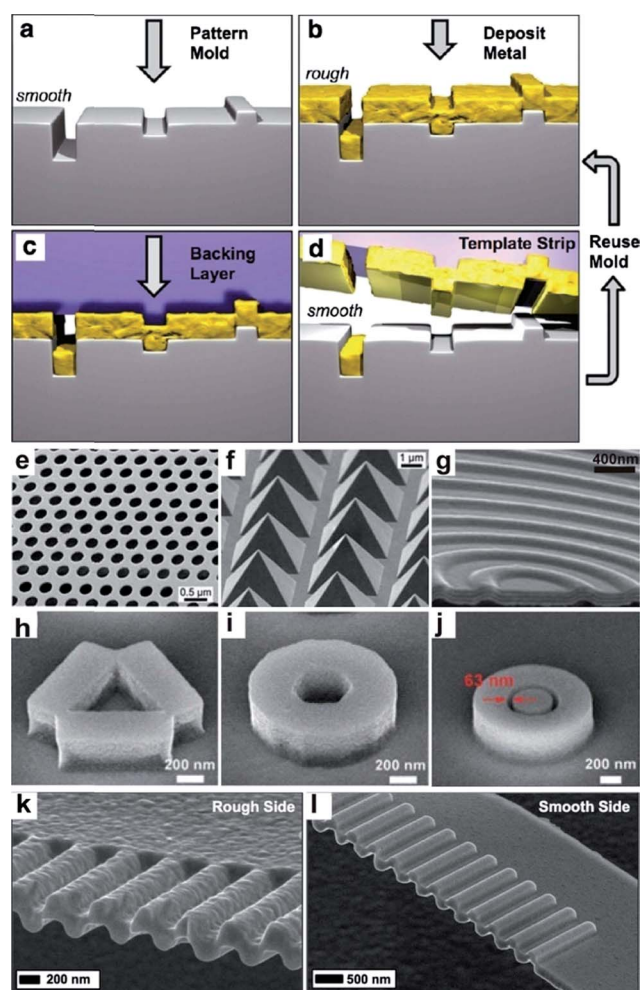


Fig. 5 Physically patterned, ultrasmooth surfaces. (a–d) Process flow for the template stripping process using a pre-patterned silicon wafer as a template.⁶² (a) Generation of patterns in the Si-wafer template; (b) deposition of gold; (c) attachment of a backing layer; (d) mechanical cleavage of the wafer: the patterns are transferred to the gold film. Discontinuous gold films lead to the creation of nanoscale holes in the template stripped substrate. (e–l) Examples of structures generated by the process. Reprinted with permission from ref. 62. Copyright 2011 American Chemical Society. (e) Nanohole film, from ref. 16. Reprinted with permission from AAAS. (f) Pyramid arrays, from ref. 16. Reprinted with permission from AAAS. (g) Multilayer bull's eye, from ref. 16. Reprinted with permission from AAAS. (h–j) Nanowells with different geometries, reprinted with permission from ref. 63; (k and l) freestanding nanoscale grooves: (k) rough side of deposited silver film; (l) template stripped, smooth side. Reprinted with permission from ref. 62. Copyright 2011 American Chemical Society.

hotspots on the sample surface. Examples will be introduced in the next chapter.

4. Applications

Imaging and investigation of surface deposited objects

Template stripped substrates are ideal to visualize and investigate nanoscopic objects deposited onto a surface. A typical example is the investigation of self-assembled monolayers. When the roughness of the interface is significantly smaller than the

dimensions of the deposited structures, structural details can be easily monitored. As an example, the orientation of alkanethiols on silver and gold surfaces has been determined using Raman spectroscopy.⁶⁵ Typically, a template stripped surface can be used as a baseline measurement to investigate the effect of surface roughness on the assembly process and on structural parameters of the assembled monolayer.^{66–69} Additionally, the effect of the surface topography on the permeability of surface films has been investigated.^{8,70–72} In general, it has been shown that a smooth interface allows for a more defined layer deposition. Self-assembled monolayers on template stripped surfaces typically form more homogeneous and more ordered films.^{8,73} The defect density is significantly reduced when compared to rougher surfaces.⁸ This leads to films with higher electrical resistances and lower capacitances. The latter is important when the surface films are to be used in electronic applications, for example thin film transistors.

Besides self-assembled monolayers, smooth template stripped surfaces have been used to image and investigate a variety of biomolecules such as two-dimensional crystals of the plant light-harvesting complex,²³ other membrane proteins⁷⁴ and biomolecules such as DNA² or proteins.⁷⁵

Finally, template stripped surfaces have been used to characterize the atomic structures of metal films by using surface tunneling microscopy (STM).²⁷ The investigation also allowed for insight into the growth mechanism of metal films during formation.³⁰

Surface force measurements

Ultraflat surfaces are typically used to image objects of nanometer dimensions deposited on top of the surface. However, such surfaces are also useful to study other surface related effects, most prominently the investigation of various surface forces. For example, template stripped gold surfaces have been used to measure the Casimir force in air.⁷⁶ A smooth interface was crucial in order to accurately measure forces between the two surfaces at small separation distances. Smooth surfaces have also been employed to determine separation forces of different materials, for example gold and mica,⁴ whereas before such measurements were limited to materials with naturally smooth interfaces.⁷⁷ The advantage of the smooth interface is that artifacts due to surface roughness can be excluded, mimicking a perfect plane much more accurately than a thermally deposited metal film.

More recently, template stripped gold surfaces have been used to measure gold/mica separation forces in solution.²³ By performing measurements in water and saline solutions, theoretical predictions from the DLVO about the interaction of charged surfaces were verified.

Structure generation

An ultra-smooth surface is also a prerequisite for the formation of nanoscopic surface architectures, which could find applications for example in microelectronics. Again, to produce functional devices with nanometer dimensions, the roughness of the surface should not exceed the dimensions of the structures. Template stripped titanium films have been used as a smooth

platform for the controlled deposition of oxide structures (Fig. 6).²¹ By using scanning probe microscopy and applying voltage modulation the surface can be oxidized in certain areas, forming three dimensional surface nanostructures. A different approach has also used a template stripped gold surface as the smooth basis to grow three dimensional polyelectrolyte structures. Using microcontact printing and a layer-by-layer deposition technique,⁶⁹ different structures such as pillars, ridges and wells could be created with very high precision and resolution (Fig. 6b). The creation of patterns of organic molecules with very high precision and feature sizes at nanoscale can be achieved by using AFM cantilevers. Dip-pen nanolithography^{91,92} uses thiols as inks that are deposited by the cantilever while nanografting techniques apply AFM cantilevers to scratch thiols off the surface at a spatially confined region.^{89,90} Both techniques are extremely powerful in the generation of structures. However, the visualization of such structures is comparably difficult as the roughness dimensions of the substrate often exceed the typical height of the organic molecules that are deposited. Template-stripped gold substrates have been successfully employed to directly visualize a variety of surface modification steps on nanografted substrates. Fig. 6c shows an example of DNA hybridization on a nanografted substrate. The line scans allow for a very clear observation of the hybridization event.⁸⁹ The confined placement of complex protein-based assemblies onto nanoscale surface patterns was demonstrated on template-stripped gold substrates as well (Fig. 6d).⁹⁰ A monolayer of

thiol-terminated polyethylene glycol was selectively removed and replaced by a positively charged thiol that allowed for selective binding of proteins. These were further used as a template to bind rabbit IgG and goat anti-rabbit IgG antibodies and antigens.

Solid supported membranes

In order to mimic the properties of a natural bilayer membrane and to study membrane related processes, solid supported model membrane systems have been established. In principle, these architectures consist of a lipid bilayer supported by a solid substrate, often mediated by an intermediate layer. These systems have been used to study fundamental membrane processes but serve also as a matrix to host membrane proteins for functional studies. In tethered bilayer lipid membranes (tBLMs), the inner membrane leaflet is attached to the solid support through a spacer equipped with an anchor group.^{6,87,88} This has been shown to lead to an increased stability of the model system compared with free-floating membranes.⁷⁸ tBLMs also have been shown to provide an electrically insulating matrix, suitable for the incorporation and study of ion channel proteins. However, in order to assure highest electrical resistances, a smooth surface is essential. Template stripped gold electrodes have been proven to allow for the formation of tBLMs with electrical resistances similar to biological lipid membranes.⁵

Template stripped heterogeneous substrates in combination with tBLMs have been used by Jung *et al.* to probe lateral

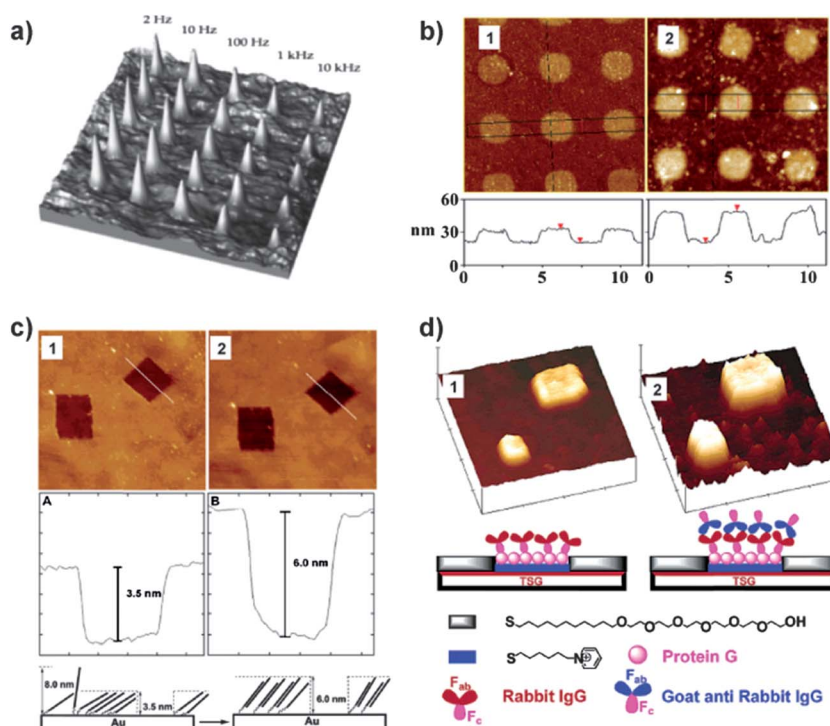


Fig. 6 Precision structure generation on template stripped substrates. (a) An example of 3D nanostructure growths on template stripped surfaces. Surface nanostructures are generated by controlled STM induced oxidation of titanium substrates. Reprinted with permission from ref. 21. (b) Polyelectrolyte microstructures obtained by microcontact printing of thiols and layer by layer deposition of polyelectrolytes. Reprinted with permission from ref. 69. Copyright 2004 American Chemical Society. (c and d) AFM induced creation of nanoscale holes in thiol monolayers and subsequent surface modifications. The low surface roughness allows for a clear visualization of the individual process steps. (c) Direct observation of DNA hybridization on nanografted holes in a single-stranded DNA monolayer. Reprinted with permission from ref. 89. Copyright 2002 American Chemical Society. (d) Protein patterning at nanoscale. Reprinted with permission from ref. 90. Copyright 2003 American Chemical Society.

dynamics in lipid membranes (Fig. 7).⁷ A substrate composed of silicon discs embedded in a gold film has been used. The gold areas have been functionalized with a tBLM using polymerizable anchor lipids, which were cross-linked by UV irradiation. When fluorescently marked lipids were fused with the cross-linked tethered monolayers, a homogeneous bilayer formed, effectively spanning the non-functionalized silicon discs. Using photobleaching techniques, the diffusion of the lipids in the outer membrane leaflet and the effective corralling of fluid lipids in the inner leaflet were observed. Fig. 7a shows the fluorescence recovery after the photobleaching experiment on the completed bilayer spanning both gold- and silicon dioxide parts of the patterned substrate. The fluorescence recovery of approximately 50% indicates the presence of a fully intact bilayer membrane with a fluid distal leaflet spanning over both gold and SiO₂ parts. When this distal leaflet was chemically bleached, no recovery after photobleaching was observed (Fig. 7b), hence proving the complete absence of diffusion of lipids into the silicon dioxide discs that are corralled by the photopolymerized lipids. The heterogeneous substrate thus allowed for an effective patterning of solid supported membranes with high precision in nanometer dimensions.⁷

Plasmonics

While most applications of the template-stripping process have been focused on the smooth nature of surface as a substrate material, it has only recently been recognized that metal structures with low surface roughness themselves possess intriguing benefits for optical and plasmonic applications.^{16,84} There are several key advantages of template-stripped gold films or nanostructures compared to their classical analogues produced by

thermal deposition of noble metals. Ultrasoother metal films effectively suppress losses of light by scattering at undefined hotspots of individual grains present in rough films and can therefore be used for high precision guiding and focusing of light inside the nanostructures.⁶¹ By virtue of the same argument, the propagation lengths of surface plasmons are dramatically increased in low-loss template-stripped gold films.¹⁶ It has also been shown that the refractive index sensitivity can be increased by eliminating surface roughness⁷⁹ and that the dielectric properties of template-stripped films are of significantly higher quality compared to thermally evaporated thin gold films.^{29,85} An additional, maybe more technical benefit of template stripped substrates is the possibility of extended storage and on-demand cleavage of samples.

Consequences for refractive index sensing

In a fundamental study on the influence of roughness in surface plasmon resonance (SPR) sensing experiments, Rueda *et al.* showed that there are significant differences between a rough and a template-stripped gold film in terms of their dielectric properties.²⁹ In standard SPR sensing experiments, widely used for the investigation of (bio)molecule adsorption,⁸⁰ these differences are neglected as the gold film is modeled as a homogeneous entity. However, it was shown that even though large errors are made by ignoring the physical reality of heterogeneity of such a gold thin film in typical data treatment, the consequences in terms of accurate determination of the thickness of deposited dielectric thin films are usually very small.²⁹

An increase in sensitivity of a sensor platform based on surface plasmon resonances was reported by Im *et al.* for silver nanohole arrays.⁷⁹ It was found that nanohole arrays fabricated by

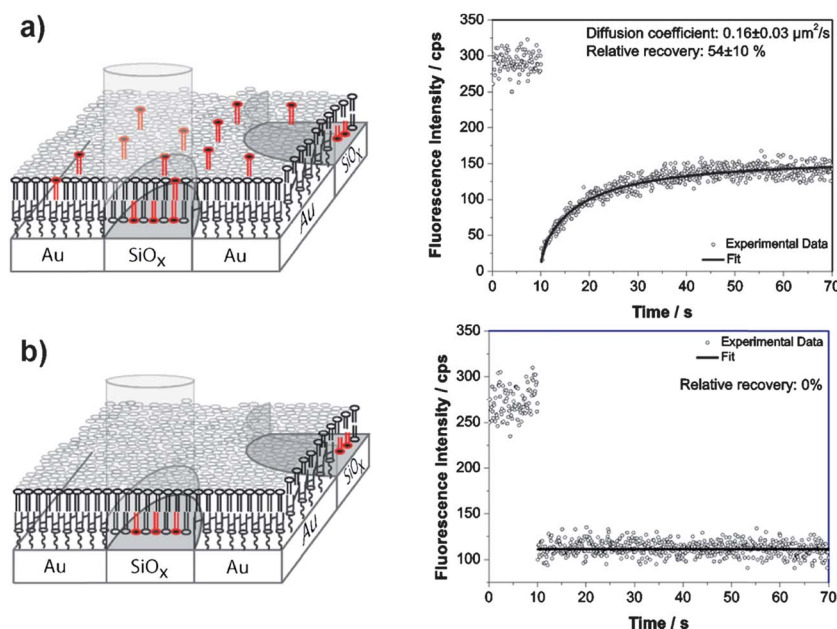


Fig. 7 A substrate consisting of silicon discs embedded in a gold film has been functionalized with a cross-linked tethered bilayer lipid membrane. Fluorescence recovery after photobleaching was used to measure diffusion coefficients and recovery in the outer and inner membrane leaflet. (a) Diffusion in both leaflets. 50% recovery indicates that the lipids in the inner leaflet cannot diffuse back in the observation spot. (b) After chemically bleaching the fluorophores in the outer leaflet and photobleaching lipids in the inner leaflet, no diffusion is observed, demonstrating the effective isolation of individual membrane patches by the diffusion barriers. Reprinted with permission from ref. 7. Copyright 2011 American Chemical Society.

template stripping from FIB engineered silicon wafer templates featured an increased refractive index sensitivity 67% higher than the rough, nanostructured silver films.

High quality nanostructures

1. Cavity modes. By creating pre-patterns of photoresist on the template wafer, Zhu *et al.* designed high quality ultra-flat metal nanostructures with a variety of shapes and feature sizes in the nanometer range and high aspect ratios (compare Fig. 5h–j).⁶³ As a consequence of the high quality of the ultra-flat metal surfaces, these metal structures support multiple, very clearly resolved cavity modes that were visualized by mono- and polychromatic cathodoluminescence (CL) spectroscopy. Fig. 8 highlights cavity mode patterns present in an equilateral triangle plasmonic cavity structure. The CL images, shown in Fig. 8a–c directly visualize the emitted photon density of three different plasmonic modes inside the nanocavity that relate well to the simulated patterns shown in Fig. 8d–f.

2. Robust structures. Embedding gold nanostructures into dielectric, ultra-flat silicon dioxide films (chemical patterning; Fig. 3) yields very robust sensing platforms. Such substrates were

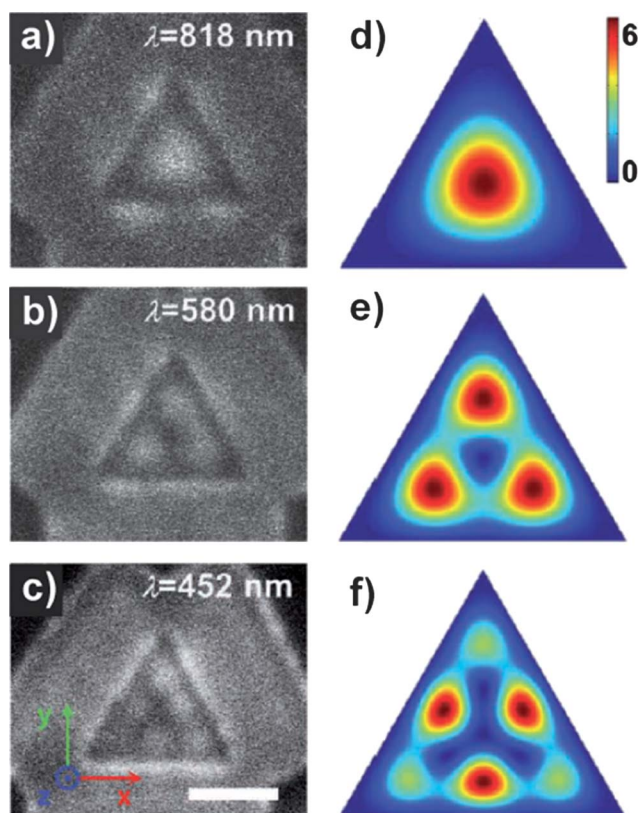


Fig. 8 Direct visualization of cavity modes by cathodoluminescence imaging in a high quality equilateral triangle plasmonic nanocavity produced by template-stripping.⁶³ (a–c) Monochromatic cathodoluminescence images of different cavity modes. The respective wavelengths are shown in the insets. Scalebars are 500 nm. The brightness corresponds to the emitted photon intensity. (d–f) Simulated mode patterns. Reprinted with permission from ref. 63.

used by Vogel *et al.* to demonstrate the re-usability of a sensor based on localized surface plasmon resonances.¹⁵ The plasmon resonances of gold nanotriangles firmly embedded into the silicon dioxide matrix by a combination of colloidal lithography and the template-stripping procedure were used to monitor the deposition of polyelectrolyte multilayers with a sensitivity comparable to conventional nanoparticle arrays prepared by colloidal lithography.⁸¹ Subsequently, the polyelectrolyte covered sensor surface was mechanically cleaned by wiping with a tissue soaked in ethanol without inducing damage to the surface-embedded nanoparticles. Thus, the sensing platform could be re-used multiple times without loss of signal intensity or sensitivity (Fig. 9a–d).¹⁵

3. Extraordinary transmission. The production of free-standing, three dimensional metallic thin films with both convex and concave features was recently demonstrated by Lindquist *et al.* who combined focused ion beam induced milling and matter deposition to produce silicon wafer templates that were patterned above- and below their surface, yielding surface structures simultaneously consisting of bumps and apertures on the template-stripped substrate.⁶² Furthermore, using micromanipulation techniques, the deposited metal films were cleaved *in situ* from the template wafer, thus giving rise to metal films with patterns on both sides (Fig. 5k and l). Such substrates are of high interest for plasmonic applications as gratings can be incorporated on both sides of the metal film with perfect alignment. This allows for simultaneous in-coupling and out-coupling of optical energy and can be used *e.g.* to support extraordinary transmission of light through optical thick metal film with nanoscale apertures. Fig. 10 exemplarily shows a bull's eye structure with a nanoscale aperture surrounded by concentric gratings. Due to the preparation process, the patterns are replicated on the other

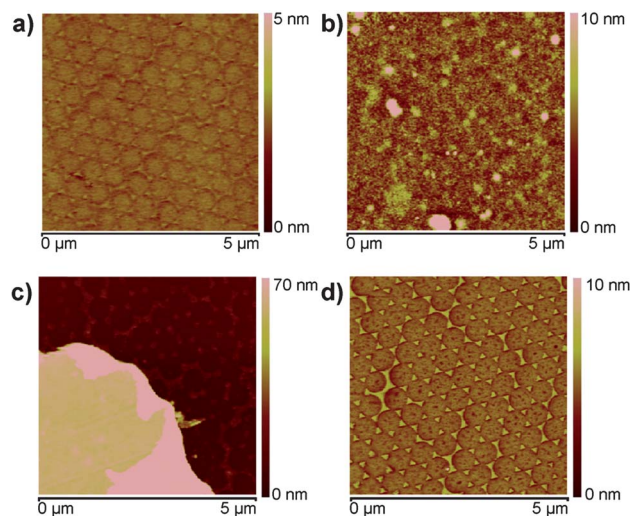


Fig. 9 A re-usable sensing platform based on surface embedded nanoparticles produced by template-stripping. The figure shows AFM height images of the substrate surface after cleaving from the template wafer (a); after layer-by-layer deposition of polyelectrolytes (b); during mechanical removal of the polymer thin film (c) and after complete recovery of the sensor substrate (d). Reprinted with permission from ref. 15.

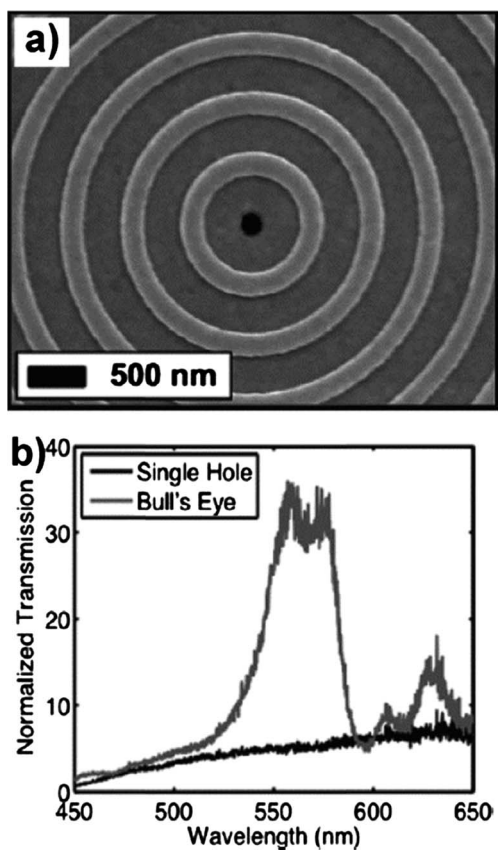


Fig. 10 Extraordinary transmission in freestanding, optically thick 3D template stripped substrates: coupling and focusing of surface plasmons onto the bull's eyes by the concentric plasmon bumps leads to strong transmission through the aperture. (a) SEM image of the bull's eye nanostructure. (b) Transmission spectra showing the enhanced transmission of light through the bull's eye nanostructure. Reprinted with permission from ref. 62. Copyright 2011 American Chemical Society.

side of the device as well, allowing for effective coupling of light into the metal film. As a consequence, the transmission of light through the aperture is boosted compared to a single aperture without the grating structure (Fig. 10b).⁶²

4. Precision hotspot engineering. The lack of topography of template-stripped gold films eliminates losses of light by scattering at undefined hotspots of individual grains. Therefore, the propagation length of surface plasmons is increased by a factor of 5–7 when compared to conventional, evaporated gold films. The plasmon propagation wavelengths measured were close to the theoretical limit of purely ohmic losses by electron scattering in the metal.¹⁶

The extraordinary smoothness of metal nanostructures engineered by template-stripping processes was used by Lindquist *et al.* to demonstrate three dimensional focusing of light in extremely small volumes using silver nanopylramids with asymmetrical gratings.⁶¹ The structures were prepared by anisotropic etching of the silicon wafer template to produce inverted pyramids. These were further processed by a focused ion beam to include nanoscale gratings at the faces of the pyramid (Fig. 11a and b). The overlay in Fig. 11a sketches the

principle of light focusing. Incident light is converted into surface plasmons that travel up the sides of the pyramids and converge at the tip. Due to the asymmetric nature of the patterning, plasmons arriving from opposite faces of the pyramid interfere constructively, giving rise to strong field confinement and enhancement. Scanning confocal Raman imaging was used to experimentally assess the focusing. Fig. 11c and d show top- and side view Raman intensity distributions of benzenethiol-covered pyramids. A single hot spot at the pyramid tip was observed in all dimensions, thus hinting at a strongly confined electric field at the tip. Without the grating structure at the faces of the pyramids, no focusing was observed (Fig. 11e). The artificial introduction of nanoscale roughness by thermal evaporation of a 100 nm silver film on top of the patterned pyramid interfered with the focusing effect (Fig. 11f), thus further underlining the importance of high quality nanostructures with extremely low roughness for next generation plasmonic devices.

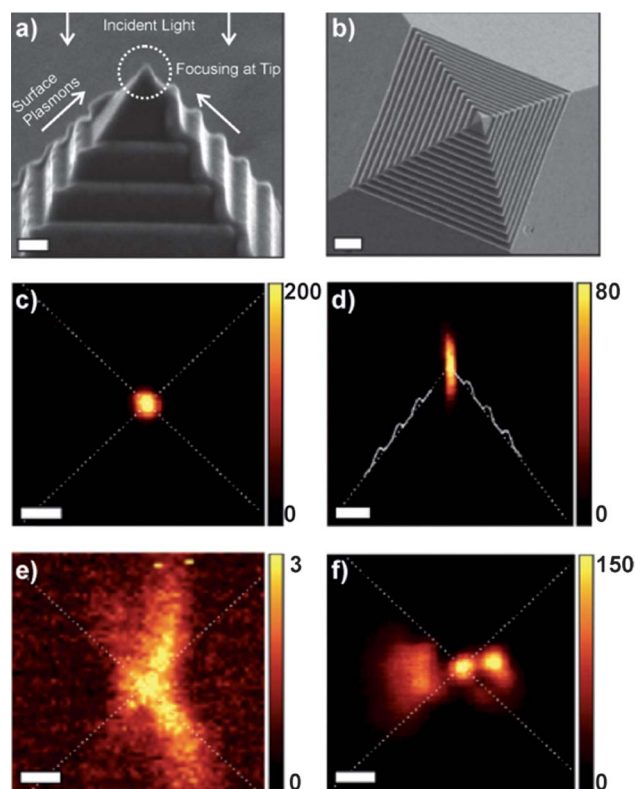


Fig. 11 Template stripped nanopylramids for nanofocusing of surface plasmons.⁶¹ (a and b) SEM micrograph of an asymmetrically patterned nanopylramid and schematic illustration of the focusing of surface plasmons at the pyramid's tip. (c–f) Scanning confocal Raman imaging. (c and d) Focusing of the Raman signal on the tip of an ultra-flat, asymmetrically patterned pyramid in top view (c) and side view (d). (e) Unpatterned nanopylramid: no focusing is observed. (f) Effect of roughness induced by evaporation of an additional silver layer onto the asymmetrically patterned pyramids: the focusing effect vanishes. Scale bars are (a) 200 nm; (b) 1000 nm; (c) 500 nm, (d) 1000 nm, (e and f) 500 nm. Reprinted with permission from ref. 61. Copyright 2011 American Chemical Society.

5. Conclusions

As miniaturization in technology continues and modern devices increasingly rely on the assembly of single molecules or monolayers thereof, surface roughness of substrates is becoming a key issue for reliable device performances. In general, the surface roughness of a substrate needs to be in the same dimension or lower as the objects to be investigated or exploited. Especially metal thin films, conventionally deposited by thermal evaporation are at risk of failing this criterion as the individual grains of the film substantially contribute to surface roughness. As a consequence, self-assembly processes of individual molecules, such as highly insulating membranes, can be compromised. Furthermore, in optical applications, undefined hotspots, formed by scattering of surface plasmons at individual grains and surface roughness features can interfere with device performances.

The template-stripping process transfers the low surface roughness of certain naturally occurring flat surfaces to a metal film, yielding a metal substrate with a surface roughness in angstrom dimensions. This article reviewed different extensions of the classical template-stripping process with respect to available templates, substrate materials to be used as well as bonding and mechanical support in an attempt to provide a versatile toolbox.

More recently, template-stripping processes for patterned substrates were reported and both the generation of material contrast in the substrate plane without any topography as well as the generation of artificial, ultrasmooth topographies by pre-patterning of a silicon wafer template became available, thus drastically expanding the range of applications of such high quality substrates.

These developments have led to an increased use of the template-stripping procedure for state-of-the-art devices in a variety of research fields; predominantly the accurate determination of surface forces, the assembly of membranes with high sealing properties as well as plasmonic applications that exploit the high quality, low loss properties of ultrasmooth metal films.

We expect to see an expansion in the use of template stripped substrates both for fundamental studies of surface bound processes as well as for sophisticated applications requiring precision-engineered substrates.

References

- 1 H. J. Butt, D. N. Wang, P. K. Hansma and W. Kuhlbrandt, *Ultramicroscopy*, 1991, **36**, 307–318.
- 2 H. J. Butt, T. Muller and H. Gross, *J. Struct. Biol.*, 1993, **110**, 127–132.
- 3 M. Hegner, P. Wagner and G. Semenza, *Surf. Sci.*, 1993, **291**, 39–46.
- 4 R. F. Knarr, R. A. Quon and T. K. Vanderlick, *Langmuir*, 1998, **14**, 6414–6418.
- 5 R. Naumann, S. M. Schiller, F. Giess, B. Grohe, K. B. Hartman, I. Karcher, I. Koper, J. Lubben, K. Vasilev and W. Knoll, *Langmuir*, 2003, **19**, 5435–5443.
- 6 I. Koper, *Mol. BioSyst.*, 2007, **3**, 651–657.
- 7 M. Jung, N. Vogel and I. Koper, *Langmuir*, 2011, **27**, 7008.
- 8 E. A. Weiss, R. C. Chiechi, G. K. Kaufman, J. K. Kriebel, Z. Li, M. Duati, M. A. Rampi and G. M. Whitesides, *J. Am. Chem. Soc.*, 2007, **129**, 4336–4349.
- 9 P. Wagner, M. Hegner, H. J. Guntherodt and G. Semenza, *Langmuir*, 1995, **11**, 3867–3875.
- 10 J. J. Blackstock, Z. Y. Li, M. R. Freeman and D. R. Stewart, *Surf. Sci.*, 2003, **546**, 87–96.
- 11 J. J. Blackstock, Z. Y. Li and G. Y. Jung, *J. Vac. Sci. Technol., A*, 2004, **22**, 602–605.
- 12 E. A. Weiss, G. K. Kaufman, J. K. Kriebel, Z. Li, R. Schalek and G. M. Whitesides, *Langmuir*, 2007, **23**, 9686–9694.
- 13 A. Alessandrini, C. A. Bortolotti, G. Bertoni, A. Vezzoli and P. Facci, *J. Phys. Chem. C*, 2008, **112**, 3747–3750.
- 14 D. Stamou, D. Gourdon, M. Liley, N. A. Burnham, A. Kulik, H. Vogel and C. Duschl, *Langmuir*, 1997, **13**, 2425–2428.
- 15 N. Vogel, M. Jung, N. L. Bocchio, M. Retsch, M. Kreiter and I. Koper, *Small*, 2010, **6**, 104–109.
- 16 P. Nagpal, N. C. Lindquist, S. H. Oh and D. J. Norris, *Science*, 2009, **325**, 594–597.
- 17 C. I. Priest, K. Jacobs and J. Ralston, *Langmuir*, 2002, **18**, 2438–2440.
- 18 L. T. Banner, A. Richter and E. Pinkhassik, *Surf. Interface Anal.*, 2009, **41**, 49–55.
- 19 C. Masens, J. Schulte, M. Phillips and S. Dligatch, *Microsc. Microanal.*, 2000, **6**, 113–120.
- 20 J. Diebel, H. Lowe, P. Samori and J. P. Rabe, *Appl. Phys. A: Mater. Sci. Process.*, 2001, **73**, 273–279.
- 21 K. Unal, B. O. Aronsson, Y. Mugnier and P. Descouts, *Surf. Interface Anal.*, 2002, **34**, 490–493.
- 22 F. F. Rossetti, I. Reviakine and M. Textor, *Langmuir*, 2003, **19**, 10116–10123.
- 23 L. Chai and J. Klein, *Langmuir*, 2007, **23**, 7777–7783.
- 24 D. Pires, B. Gotsmann, F. Porro, D. Wiesmann, U. Duerig and A. Knoll, *Langmuir*, 2009, **25**, 5141–5145.
- 25 B. Atmaja, J. Frommer and J. C. Scott, *Langmuir*, 2006, **22**, 4734–4740.
- 26 D. W. Mosley, B. Y. Chow and J. A. Jacobson, *Langmuir*, 2006, **22**, 2437–2440.
- 27 P. Samori, J. Diebel, H. Lowe and J. P. Rabe, *Langmuir*, 1999, **15**, 2592–2594.
- 28 P. Gupta, K. Loos, A. Korniaikov, C. Spagnoli, M. Cowman and A. Ulman, *Angew. Chem., Int. Ed.*, 2004, **43**, 520–523.
- 29 A. Rueda, N. Vogel and M. Kreiter, *Surf. Sci.*, 2009, **603**, 491–497.
- 30 R. Ragan, D. Ohlberg, J. J. Blackstock, S. Kim and R. S. Williams, *J. Phys. Chem. B*, 2004, **108**, 20187–20192.
- 31 S. Borukhin and B. Pokroy, *Langmuir*, 2011, **27**, 13415–13419.
- 32 A. Kumar and G. M. Whitesides, *Appl. Phys. Lett.*, 1993, **63**, 2002–2004.
- 33 Y. N. Xia and G. M. Whitesides, *Annu. Rev. Mater. Sci.*, 1998, **28**, 153–184.
- 34 Y. N. Xia, J. A. Rogers, K. E. Paul and G. M. Whitesides, *Chem. Rev.*, 1999, **99**, 1823–1848.
- 35 U. Jonas, A. del Campo, C. Kruger, G. Glasser and D. Boos, *Proc. Natl. Acad. Sci. U. S. A.*, 2002, **99**, 5034–5039.
- 36 A. del Campo, D. Boos, H. W. Spiess and U. Jonas, *Angew. Chem., Int. Ed.*, 2005, **44**, 4707–4712.
- 37 V. San Miguel, C. G. Bochet and A. del Campo, *J. Am. Chem. Soc.*, 2011, **133**, 5380–5388.
- 38 X. Y. Zhang, A. V. Whitney, J. Zhao, E. M. Hicks and R. P. Van Duyne, *J. Nanosci. Nanotechnol.*, 2006, **6**, 1920–1934.
- 39 J. H. Zhang, Y. F. Li, X. M. Zhang and B. Yang, *Adv. Mater.*, 2010, **22**, 4249–4269.
- 40 N. Vogel, C. K. Weiss and K. Landfester, *Soft Matter*, 2012, **8**, 4044.
- 41 W. Frey, C. K. Woods and A. Chilkoti, *Adv. Mater.*, 2000, **12**, 1515–1519.
- 42 B. Jung and W. Frey, *Nanotechnology*, 2008, **19**, 145303.
- 43 N. Vogel, M. Jung, M. Retsch, W. Knoll, U. Jonas and I. Koper, *Small*, 2009, **5**, 821–825.
- 44 J. P. Wright, O. Worsfold, C. Whitehouse and M. Himmelhaus, *Adv. Mater.*, 2006, **18**, 421.
- 45 J. C. Hulteen, D. A. Treichel, M. T. Smith, M. L. Duval, T. R. Jensen and R. P. Van Duyne, *J. Phys. Chem. B*, 1999, **103**, 3854–3863.
- 46 J. C. Hulteen and R. P. Van Duyne, *J. Vac. Sci. Technol., A*, 1995, **13**, 1553–1558.
- 47 M. R. Jones, K. D. Osberg, R. J. Macfarlane, M. R. Langille and C. A. Mirkin, *Chem. Rev.*, 2011, **111**, 3736–3827.
- 48 N. Vogel, L. de Viguierie, U. Jonas, C. Weiss and K. Landfester, *Adv. Funct. Mater.*, 2011, **21**, 3064.
- 49 N. Vogel, S. Goerres, C. K. Weiss and K. Landfester, *Macromol. Chem. Phys.*, 2011, **212**, 1719.

- 50 A. Kosiorek, W. Kandulski, H. Glaczynska and M. Giersig, *Small*, 2005, **1**, 439–444.
- 51 M. Retsch, M. Tamm, N. Bocchio, N. Horn, R. Forch, U. Jonas and M. Kreiter, *Small*, 2009, **5**, 2105–2110.
- 52 M. Bayati, P. Patoka, M. Giersig and E. R. Savinova, *Langmuir*, 2010, **26**, 3549–3554.
- 53 J. Fischer, N. Vogel, R. Mohammadi, H. J. Butt, K. Landfester, C. K. Weiss and M. Kreiter, *Nanoscale*, 2011, **3**, 4788.
- 54 N. Vogel, J. Fischer, R. Mohammadi, M. Retsch, H. J. Butt, K. Landfester, C. K. Weiss and M. Kreiter, *Nano Lett.*, 2011, **11**, 446–454.
- 55 J. R. Jeong, S. Kim, S. H. Kim, J. A. C. Bland, S. C. Shin and S. M. Yang, *Small*, 2007, **3**, 1529–1533.
- 56 A. Manzke, A. Plettl, U. Wiedwald, L. Han, P. Ziemann, E. Schreiber, U. Ziener, N. Vogel, K. Landfester, K. Fauth, J. Biskupek and U. Kaiser, *Chem. Mater.*, 2012, **24**, 1048.
- 57 G. Kastle, H. G. Boyen, F. Weigl, G. Lengel, T. Herzog, P. Ziemann, S. Riethmuller, O. Mayer, C. Hartmann, J. P. Spatz, M. Moller, M. Ozawa, F. Banhart, M. G. Garnier and P. Oelhafen, *Adv. Funct. Mater.*, 2003, **13**, 853–861.
- 58 J. P. Spatz, S. Mossmer, C. Hartmann, M. Moller, T. Herzog, M. Krieger, H. G. Boyen, P. Ziemann and B. Kabius, *Langmuir*, 2000, **16**, 407–415.
- 59 A. Manzke, N. Vogel, C. K. Weiss, U. Ziener, A. Plettl, K. Landfester and P. Ziemann, *Nanoscale*, 2011, **3**, 2523.
- 60 N. Vogel, C. P. Hauser, K. Schuller, K. Landfester and C. K. Weiss, *Macromol. Chem. Phys.*, 2010, **211**, 1355.
- 61 N. C. Lindquist, P. Nagpal, A. Lesuffleur, D. J. Norris and S.-H. Oh, *Nano Lett.*, 2010, **10**, 1369–1373.
- 62 N. C. Lindquist, T. W. Johnson, D. J. Norris and S.-H. Oh, *Nano Lett.*, 2011, **11**, 3526.
- 63 X. L. Zhu, Y. Zhang, J. S. Zhang, J. Xu, Y. Ma, Z. Y. Li and D. P. Yu, *Adv. Mater.*, 2010, **22**, 4345.
- 64 K. W. Kho, Z. X. Shen and M. Olivo, *Opt. Express*, 2011, **19**, 10518–10535.
- 65 M. A. Bryant and J. E. Pemberton, *J. Am. Chem. Soc.*, 1991, **113**, 8284–8293.
- 66 L. H. Guo, J. S. Facci, G. McLendon and R. Mosher, *Langmuir*, 1994, **10**, 4588–4593.
- 67 J. S. Huang, V. Callegari, P. Geisler, C. Bruning, J. Kern, J. C. Prangma, X. F. Wu, T. Feichtner, J. Ziegler, P. Weinmann, M. Kamp, A. Forchel, P. Biagioni, U. Sennhauser and B. Hecht, *Nat. Commun.*, 2010, **1**, 150.
- 68 M. S. Miller, R. R. S. Juan, M.-A. Ferrato and T. B. Carmichael, *Langmuir*, 2011, **27**, 10019–10026.
- 69 D. Zhou, A. Bruckbauer, M. Batchelor, D.-J. Kang, C. Abell and D. Klenerman, *Langmuir*, 2004, **20**, 9089–9094.
- 70 M. C. Leopold, J. A. Black and E. F. Bowden, *Langmuir*, 2002, **18**, 978–980.
- 71 J. W. Ciszek and J. M. Tour, *Chem. Mater.*, 2005, **17**, 5684–5690.
- 72 V. B. Engelkes, J. M. Beebe and C. D. Frisbie, *J. Phys. Chem. B*, 2005, **109**, 16801–16810.
- 73 S. Lee, S.-S. Bae, G. Medeiros-Ribeiro, J. J. Blackstock, S. Kim, D. R. Stewart and R. Ragan, *Langmuir*, 2008, **24**, 5984–5987.
- 74 P. L. T. M. Frederix, P. D. Bosshart and A. Engel, *Biophys. J.*, 2009, **96**, 329–338.
- 75 D. Losic, J. G. Shapter and J. J. Gooding, *Aust. J. Chem.*, 2001, **54**, 643–648.
- 76 T. Ederth, *Phys. Rev. A*, 2000, **62**, 062104.
- 77 R. G. Horn, J. N. Israelachvili and F. Pribac, *J. Colloid Interface Sci.*, 1987, **115**, 480–492.
- 78 I. K. Vockenroth, C. Ohm, J. W. F. Robertson, D. J. McGillivray, M. Losche and I. Koper, *Biointerphases*, 2008, **3**, FA68–FA73.
- 79 H. Im, S. H. Lee, N. J. Wittenberg, T. W. Johnson, N. C. Lindquist, P. Nagpal, D. J. Norris and S.-H. Oh, *ACS Nano*, 2011, **5**, 6244–6253.
- 80 W. Knoll, *Annu. Rev. Phys. Chem.*, 1998, **49**, 569–638.
- 81 A. J. Haes, S. L. Zou, G. C. Schatz and R. P. Van Duyne, *J. Phys. Chem. B*, 2004, **108**, 109–116.
- 82 P. Cacciafesta, A. D. L. Humphris, K. D. Jandt and M. J. Miles, *Langmuir*, 2000, **16**, 8167–8175.
- 83 P. Cacciafesta, K. R. Hallam, C. A. Oyedepo, A. D. L. Humphris, M. J. Miles and K. D. Jandt, *Chem. Mater.*, 2002, **14**, 777–789.
- 84 C. L. Nathan, N. Prashant, M. M. Kevin, J. N. David and O. Sang-Hyun, *Rep. Prog. Phys.*, 2012, **75**, 036501.
- 85 J. H. Park, P. Nagpal, S. H. Oh and D. J. Norris, *Appl. Phys. Lett.*, 2012, **100**, 081105.
- 86 J. T. Hugall, A. S. Finmore, J. J. Baumberg, U. Steiner and S. Mahajan, *Langmuir*, 2011, **28**, 1347–1350.
- 87 X. Wang, M. M. Shindel, S.-W. Wang and R. Ragan, *Langmuir*, 2010, **26**, 18239–18245.
- 88 V. Atanasov, P. P. Atanasova, I. K. Vockenroth, N. Knorr and I. Köper, *Bioconjugate Chem.*, 2006, **17**, 631–637.
- 89 D. Zhou, K. Sinniah, C. Abell and T. Rayment, *Langmuir*, 2002, **18**, 8278–8281.
- 90 D. Zhou, X. Wang, L. Birch, T. Rayment and C. Abell, *Langmuir*, 2003, **19**, 10557–10562.
- 91 R. D. Piner, J. Zhu, F. Xu, S. H. Hong and C. A. Mirkin, *Science*, 1999, **283**, 661–663.
- 92 A. Baserga, M. Viganò, C. S. Casari, S. Turri, A. Li Bassi, M. Levi and C. E. Bottani, *Langmuir*, 2008, **24**, 13212–13217.